Energy and autoionization width of the $1s3s3p\ ^4P^\circ$ and $1s3p3p\ ^4P$ states in lithiumlike ions

Brian F. Davis
Department of Physics, University of North Carolina at Wilmington, Wilmington, North Carolina 28403

Kwong T. Chung
Department of Physics, North Carolina State University, Raleigh, North Carolina 27695
and Institute of Atomic and Molecular Sciences, Academia Sinica, Taipei, Taiwan 10764, Republic of China
(Received 13 November 1989)

The saddle-point complex-rotation method is used to compute the energies and autoionization widths of the $1s3s3p\ ^4P^\circ$ and $1s3p3p\ ^4P$ Feshbach resonances for the lithiumlike ions with nuclear charges from $Z=2$ to 6. These doubly core-excited quartet states rapidly autoionize, emitting low-energy electrons via the continua associated with the $1s2s\ ^3S$ and $1s2p\ ^3P^\circ$ states of the residual ion. The radiative decay rates of these initial states are shown to be small relative to their autoionization rates, so that the lifetimes of these resonances are essentially determined by their widths due to autoionization. A detailed study of the closed-channel component of the $1s3p3p\ ^4P$ resonance is made in order to investigate the degree to which the saddle-point solution approximates this component of the resonance wave function.

I. INTRODUCTION

The $1s3s3p\ ^4P^\circ$ and $1s3p3p\ ^4P$ states in lithiumlike systems are Feshbach resonances that for small values of the nuclear charge Z decay predominantly by autoionization. These systems are closed-channel resonances with respect to the excited two-electron target states $1s3s\ ^3S$ and $1s3p\ ^3P^\circ$. The energies of both these resonances lie below both the $1s3s\ ^3S$ and $1s3p\ ^3P^\circ$ closed-channel target states, except for the negative ion $1s3p3p\ ^4P^\circ$ state in He^-, which lies above the $1s3s\ ^3S$ threshold of He. The Auger energies of the electrons emitted by these doubly excited states is small compared to those doubly excited states in the elastic-scattering energy region. The Auger energy associated with the decay of the $[1s(2s2p)^3P]^2P^\circ$ state[1] for instance is an order of magnitude larger for the case of Be^+ as compared to those Be^+ systems being studied here. Resonances positioned above the first excited-state threshold of the target system $1s2s\ ^3S$ emit lower energy electrons; an example is the lithium spectrum[2] where Auger energies lower than those studied here were measured and identified with the decay of the $[(1s2p)^3P^\circ,3p]^4D$, $[(1s2p)^3P^\circ,3p]^4S$, and $[(1s2p)^3P^\circ,3d]^4F^\circ$ states. The well-studied lithiumlike quartet systems, $1s2p2p\ ^4P$ (Ref. 3) and $1s2s2p\ ^4P^\circ$,[4] contrast with those studied here in that they are spin forbidden to autoionize in the nonrelativistic approximation. They can couple to the continua associated with the $1s1s\ ^1S$ state of the target system only through the magnetic spin-dependent interactions. The $1s3s3p\ ^4P^\circ$ and $1s3p3p\ ^4P$ states on the other hand couple to the continua associated with the $1s2s\ ^3S$ and $1s2p\ ^3P^\circ$ states via the Coulomb interaction and therefore autoionize quite rapidly. The radiative rates for decay from these quartet states are much smaller than the autoionization rates, making these states essentially optically unobservable for small Z.

The calculation of the energies and wave functions of the $1s2s2p\ ^4P^\circ$ and $1s2p2p\ ^4P$ states is simple with a variational approach since they behave as bound states, and as a result satisfy the upper-bound property. The inner-shell vacancies in these states are implicitly present as a result of the Pauli antisymmetry principle. On the other hand, the vacancies in the $1s3s3p\ ^4P^\circ$ and $1s3p3p\ ^4P$ states must be included in the trial wave function explicitly. The saddle-point variational method is utilized in this work to explicitly include all the relevant inner-shell vacancies into the closed-channel wave function. This method gives a good approximation for the energy of a narrow Feshbach resonance. The full resonant wave function is investigated for the purpose of computing autoionization widths by including the open-channel component through the use of complex coordinates. This saddle-point complex-rotation method is used at two different levels of approximation.[5] We find that correlation effects for the very-low-Z systems necessitate the use of a trial wave function which is flexible enough so that the closed-channel and open-channel components of the full resonant wave function can interact and consequently influence each other's structure in the variation calculation.

II. CLOSED-CHANNEL WAVE FUNCTION—THE SADDLE-POINT METHOD

The saddle-point technique is a variational method which is used to obtain the best square-integrable wave-function approximation for inner-shell vacancy states in atomic systems.[6] However, if the energy of the inner-shell vacancy state is degenerate with a continuum of the same angular and spin symmetry, then the full resonance

wave function will contain an open-channel component which includes this continuum. The saddle-point wave function can then be considered the closed-channel component of this full resonant wave function. We have found, for narrow Feshbach resonances, that the saddle-point energy is usually a good approximation to the resonance energy from which Auger energies are computed and compared with experiment.[7] A golden-rule analysis of the resonance width via perturbation theory basically yields an expression of the following form:[8]

$$\Gamma=\hbar T \quad \text{with } T=\frac{2\pi}{\hbar}|\langle\psi_f|\mathcal{H}-E|\psi_i\rangle|^2\rho(\varepsilon)\ . \tag{1}$$

Here Γ is the autoionization width, T is the transition rate, ψ_i and ψ_f are the wave functions of the initial and final states, respectively, and $\rho(\varepsilon)$ is the energy density of final states. An isoelectronic analysis of the width given by this expression for a given resonance as a function of Z where products of hydrogenic wave functions are used for the initial and final states yields a result[9] which is independent of Z. We have observed this trend to be approximately true in earlier works where the widths were computed independently for each value of the nuclear charge with the saddle-point complex-rotation method. Examples may be seen in Tables II and III of Ref. 3 for the $1s2p2p\ ^2D$ and $1s2p2p\ ^2S$ resonances, respectively, and in Tables II and III of Ref. 4 for the $[1s(2s2p)^3P]^2P^\circ$ and $[1s(2s2p)^1P]^2P^\circ$ resonances, respectively. These examples also illustrate that the widths for small values of Z are not independent of Z. This is to be expected, however, since nuclear screening effects and electron-electron interactions in the low-Z systems act to significantly perturb the electron orbitals from the hydrogenic forms relative to high-Z systems. These correlation effects have bearing on whether or not Eq. (1) is a valid approximation. Consider the same transition for small and large values of Z from the point of view of Eq. (1). If the results for the widths are comparable in magnitude, then the interactions between the electrons in the low-Z system are much larger relative to the electron-nucleus interactions. When this is the case, then the correlation effects are large, and a determination of the full resonant wave function will reveal that the open- and closed-channel components can modify each other to the point that the original initial and final state decomposition is not accurate.

The basis functions used in these saddle-point calculations are eigenfunctions of L^2, L_z, S^2, and S_z and are of the following form:

$$\begin{aligned}\phi^{m,n,k}_{[(l_1,l_2)L_{12},l_3]}=&\mathcal{R}^{m,n,k}_{\alpha_\ell,\beta_\ell,\gamma_\ell}(r_1,r_2,r_3)\\ &\times\mathcal{Y}^{L,M}_{[(l_1,l_2)L_{12},l_3]}(\hat{\mathbf{r}}_1,\hat{\mathbf{r}}_2,\hat{\mathbf{r}}_3)\\ &\times\chi(\sigma_1,\sigma_2,\sigma_3)\ ,\end{aligned} \tag{2}$$

where the radial, angular, and spin parts are given, respectively, by

$$\mathcal{R}^{m,n,k}_{\alpha_\ell,\beta_\ell,\gamma_\ell}(r_1,r_2,r_3)=r_1^n r_2^m r_3^k e^{-\alpha_\ell r_1}e^{-\beta_\ell r_2}e^{-\gamma_\ell r_3}\ , \tag{3}$$

$$\mathcal{Y}^{L,M}_{[(l_1,l_2)L_{12},l_3]}(\hat{\mathbf{r}}_1,\hat{\mathbf{r}}_2,\hat{\mathbf{r}}_3)=\sum_{m_1,m_2,\mu,m_3}\langle l_1l_2m_1m_2|L_{12}\mu\rangle Y_{l_1}^{m_1}(\hat{\mathbf{r}}_1)Y_{l_2}^{m_2}(\hat{\mathbf{r}}_2)Y_{l_3}^{m_3}(\hat{\mathbf{r}}_3)\langle L_{12}l_3\mu m_3|LM\rangle\ , \tag{4}$$

$$\chi(\sigma_1,\sigma_2,\sigma_3)=\alpha(1)\alpha(2)\alpha(3)\ . \tag{5}$$

The subscript ℓ on the nonlinear variation parameters α, β, and γ refers to the particular angular partial wave, $[(l_1,l_2)L_{12},l_3]$, with which these parameters are associated. Each partial wave has one such set of nonlinear parameters which are determined by the minimization of the energy. The notation indicates that the individual angular momenta of electrons one and two, l_1 and l_2, couple to a $^3L_{12}$ state which couples to the angular momentum of the third electron l_3 to form the ^4L quartet state of interest. The same notation is used for the Clebsh-Gordan coefficients in Eq. (4). The α in Eq. (5) is the spin-up spinor.

Vacancies are built directly into the trial wave function with single-particle projection operators

$$\mathcal{P}_{nlm}(\mathbf{r})=|\phi_{nlm}(\mathbf{r})\rangle\langle\phi_{nlm}(\mathbf{r})|\ , \tag{6}$$

where

$$\phi_{nlm}(\mathbf{r})=R^{q_{nl}}_{nl}(r)Y_{lm}(\hat{\mathbf{r}})\ . \tag{7}$$

The radial part of this vacancy orbital is normalized and given by

$$R^{q_{nl}}_{nl}(r)=A_{nl}\left[\frac{2q_{nl}}{n}\right]^{3/2}e^{-q_{nl}r/n}\left[\frac{2q_{nl}r}{n}\right]^{l}F^{q}_{nl}(r) \tag{8}$$

where q_{nl} is a nonlinear variational parameter, F^q_{nl} is a polynomial of the degree $n-l-1$ in r which may depend parametrically on the vacancy-orbital parameters, and

$$A_{nl}=\left[\frac{(n-l-1)!}{2n[(n+l)!]^3}\right]^{1/2}\ . \tag{9}$$

The value of q_{nl} is determined by the saddle-point optimization procedure in which the energy of the inner-shell vacancy state is maximized with respect to those parameters in the vacancy orbitals. The explicit functional form of F^q_{nl} is determined by the requirement that the set of vacancy orbitals in a given inner-shell vacancy state be mutually orthonormal. This will be made clear by way of the examples given in this work.

The $1s3s3p\ ^4P^\circ$ saddle-point trial wave function with $1s$ and $2s$ vacancies for electron 2 and a $2p$ vacancy for electron 3 is given by

$$\Psi_q = \mathcal{A}[1-\mathcal{P}_{1s}(\mathbf{r}_2)-\mathcal{P}_{2s}(\mathbf{r}_2)]\left[1-\sum_m \mathcal{P}_{2pm}(\mathbf{r}_3)\right] \times \sum_{[\ell],i} A_{[\ell],i}\phi^{m,n,k}_{[(l_1,l_2)L_{12},l_3]} . \quad (10)$$

The vacancy orbitals ϕ_{1s} and ϕ_{2s} in $\mathcal{P}_{1s}$ and $\mathcal{P}_{2s}$ are orthogonal. $\mathcal{A}$ is the antisymmetrization operator. The summation is over the Slater-like basis functions corresponding to the powers of r, $i=(m,n,k)$, with angular symmetry $[\ell]=[(l_1,l_2)L_{12}l_3]$. The projection operators in Eq. (9) affect only the radial part of the basis; this is because

$$\sum_{m=-l}^{l} \mathcal{P}_{nlm}(\mathbf{r}_j) = \sum_{m=-l}^{l} |R^{q_{nl}}_{nl}(r_j)Y^m_l(\hat{\mathbf{r}}_j)\rangle\langle R^{q_{nl}}_{nl}(r_j)Y^m_l(\hat{\mathbf{r}}_j)| \quad (11)$$

and

$$\sum_{m=-l}^{l} |Y^m_l(\hat{\mathbf{r}}_j)\rangle\langle Y^m_l(\hat{\mathbf{r}}_j)|[(l_1,l_2)L_{12},l_3]LM\rangle = \delta_{ll_j}|[(l_1,l_2)L_{12},l_3]LM\rangle . \quad (12)$$

The vacancy orbital does not contain a spin coordinate; this is because inner-shell vacancy states are formed by orbital excitations; the correct spin eigenfunctions are assumed in the trial wave function.

The $1s3p3p\ ^4P$ saddle-point trial wave function with $2p$ vacancies for electrons 2 and 3 is given by

$$\Psi_q = \mathcal{A}\left[1-\sum_m \mathcal{P}_{2pm}(\mathbf{r}_2)\right]\left[1-\sum_m \mathcal{P}_{2pm}(\mathbf{r}_3)\right] \times \sum_{[\ell],i} A_{[\ell],i}\phi^{m,n,k}_{[(l_1,l_2)L_{12},l_3]} . \quad (13)$$

The saddle-point variation is carried out by

$$\delta\frac{\langle\Psi_q|\mathcal{H}|\Psi_q\rangle}{\langle\Psi_q|\Psi_q\rangle}=0 , \quad (14)$$

where $\mathcal{H}$ is the nonrelativistic Hamiltonian

$$\mathcal{H}=-\sum_{i=1}^{3}\left[\tfrac{1}{2}\nabla_i^2+\frac{Z}{r_i}\right]+\sum_{i<j}^{3}\frac{1}{r_{ij}} . \quad (15)$$

More explicitly the saddle-point method minimizes the energy with respect to the parameters in the electron orbitals: the linear parameters $A_{[\ell],i}$ and the nonlinear parameters $(\alpha_\ell,\beta_\ell,\gamma_\ell)$, and maximizes the energy with respect to the parameters in the vacancy orbitals q_{nl}.

Special consideration must be afforded to the $1s$ vacancy in the $1s3s3p\ ^4P^\circ$ wave function. The reason stems from the presence of a $1s$ electron in this system and the Pauli antisymmetry principle. Consider for the moment a trial wave function with the symmetry of Eq. (10), but with no projected vacancies. The process of antisymmetrization itself implicitly generates a $1s$ vacancy, i.e., the lowest root of the secular equation, Eq. (14), would be the $1s2s2p\ ^4P^\circ$ state. Therefore one might initially suppose that the $1s$ projection in Eq. (9) is unnecessary for the $1s3s3p\ ^4P^\circ$ state and only the $2s$ and $2p$ vacancies are essential. This premise would lead, however, to a variational breakdown: the resulting variation would mold electron 2 into a $1s$ electron (since we only required that it not be in a $2s$ orbital) and electron 1 would then become a $2s$ electron as a result of the Pauli antisymmetry principle. With these considerations in mind we may evaluate the requirement of the explicit presence of the $1s$ vacancy orbital in the trial wave function as virtual, the only use of which is to maintain the identity and integrity of the $1s$-electron orbital. A previous study[10] of this situation in two-electron bound states ($1s3s\ ^3S$ is one example) has led us to the conclusion that the energy must only be required to be stationary with respect to variations in the "virtual $1s$ vacancy" orbital. The investigation of the $1s3s3p\ ^4P^\circ$ system in this work has revealed that the stationary energy is a maximum with respect to

TABLE I. Energy and width of the $1s3p3p\ ^4P$ resonances in lithium-like ions. $\langle H_1+H_2\rangle$, $\langle H_4\rangle$, and $\langle H_5\rangle$ are the expectation values of the relativistic operators corresponding to kinetic energy correction plus Darwin term, orbit-orbit or retardation, and the nonrelativistic mass polarization effect, respectively. E total is the sum of the saddle-point energy (nonrelativistic energy) plus the aforementioned corrections. The shift and width results correspond to computations from the saddle-point complex-rotation method: the first results quoted (top of the line) are from the flexible-type wave function [Eq. (21)], and the second set of results (bottom of line) are from the fixed-type wave function [Eq. (20)]. The width from the flexible-type wave function is more reliable. The Auger energies are computed from E total and the shift resulting from the flexible-type wave functions. The results are quoted in atomic units, except for the Auger energies which are quoted in electron volts [see Eq. (27)].

Z	E saddle point	q_{2p}	$\langle H_1+H_2\rangle$ (units of 10^{-4})	$\langle H_4\rangle$ (units of 10^{-4})	$\langle H_5\rangle$ (units of 10^{-4})	E total	Δ shift (units of 10^{-4})	Γ width (units of 10^{-3})	ε Auger energy (eV)
2	−2.064 499	0.976	−1.07	+0.005	−0.020	−2.064 607	−5.3	1.213	1.854
							−3.8	0.678	
3	−4.846 711	1.989	−5.47	+0.052	−0.079	−4.847 261	+0.01	4.614	4.925 36
							−2.54	4.128	
4	−8.852 839	3.005	−17.54	+0.182	−0.157	−8.854 591	+4.33	5.365	8.777 70
							+2.65	5.221	
5	−14.081 796	4.017	−43.32	+0.432	−0.240	−14.086 109	+6.55	5.683	13.3889
							+5.50	5.630	
6	−20.533 261	5.024	−90.79	+0.841	−0.352	−20.542 291	+7.83	5.858	18.7572
							+7.13	5.836	

TABLE II. Energy and widths of the $1s3s3p\ ^4P^\circ$ resonances in lithiumlike Ions $\langle H_1+H_2\rangle$, $\langle H_4\rangle$, and $\langle H_5\rangle$ are the expectation values of the relativistic opertors corresponding to kinetic energy correction plus Darwin term, orbit-orbit or retardation, and the nonrelativistic mass polarization effect, respectively. E total is the sum of the saddle-point energy (nonrelativistic energy) plus the aforementioned corrections. Partial widths and shifts from both the $(1s2s\ ^3S,\varepsilon p)^4P^\circ$ and the $(1s2p\ ^3P,\varepsilon s)^4P^\circ$ continua are quoted. These shift and width results correspond to computations from the saddle-point complex-rotation method: the 1st results quoted (top of the line) are from the flexible-type wave function (Eq.21), and the 2nd set of results (bottom of line) are from the fixed-type function [Eq. (20)]. The total width is obtained by summing the partial widths (resulting from the flexible-type wave function). The Auger energies are computed from E total and the shifts resulting from the flexible-type wave functions [Eqs. (25) and (26)]. The results are quoted in atomic units, except for the Auger energies which are quoted in electron volts [See Eq. (27)].

Z	E saddle point	q_{1s} q_{2s} q_{2p}	$\langle H_1+H_2\rangle$ (units of 10^{-4})	$\langle H_2\rangle$ (units of 10^{-4})	$\langle H_5\rangle$ (units of 10^{-4})	E total and Γ total	Δ_S and Γ_S from $(1s2s\ ^3S,\varepsilon p)^4P^\circ$ (units of 10^{-4})	(units of 10^{-3})	Δ_P and Γ_P from $(1s2p\ ^3P,\varepsilon s)^4P^\circ$ (units of 10^{-4})	(units of 10^{-3})	ε_S and ε_P in eV
2	−2.075 940	1.925	−1.08	0.004	−0.020	−2.076 049	+0.96	0.2570	+1.03	1.292	2.707 00
		1.2950				0.001 549	+0.89	0.2568	−0.39	1.080	1.562 48
		0.9180									
3	−4.878 651	2.9750	−5.61	0.031	−0.053	−4.879 214	+2.60	0.9832	+3.05	1.466	6.331 40
		2.2745				0.002 449	+2.36	0.9883	+2.55	1.469	4.071 29
		1.9820									
4	−8.905 137	3.975	−18.13	0.103	−0.106	−8.906 950	+3.92	1.235	+3.61	1.517	10.6928
		3.2714				0.002 752	+3.76	1.245	+3.39	1.527	7.361 73
		3.014									
5	−14.154 271	4.965	−44.95	0.238	−0.138	−14.158 756	+4.65	1.338	+3.95	1.558	15.8091
		4.2714				0.002 896	+4.55	1.347	+3.81	1.566	11.4177
		4.032									
6	−20.625 824	5.965	−94.17	0.460	−0.199	−20.635 215	+5.08	1.387	+4.19	1.588	21.6860
		5.2714				0.002 975	+5.01	1.395	+4.10	1.596	16.2327
		5.044									

variations of q_{1s} for $Z \geq 3$, and it is a point of inflection for the He^- system.

It is worthwhile to discuss the nature of the functional form of the radial part F_{nl}^q. For the $1s3s3p\ ^4P^\circ$ system, for example, we first assume a hydrogenic $1s$-vacancy orbital whose form is determined by Eqs. (7)–(9) with $n=1$, $l=0$ and $F_{1s}=1$, i.e., the associated Laguerre polynomial.[11] The $2s$-vacancy orbital is then determined by $n=2$, $l=0$, and F_{2s}^q being the $(n-l-1)=1$st-order polynomial in r determined wholly by requiring orthogonality between ϕ_{1s} and ϕ_{2s}. This function will then only be the Laguerre polynomial if $q_{1s}=q_{2s}$, which in general is not the case. For the case under discussion here we find that $q_{1s}\approx Z$ and $q_{2s}\approx Z-1$. It is interesting to note that in the case of the $1s3s3p\ ^2P^\circ$ doublet system we would find $q_{1s}\approx Z-\frac{1}{2}$ and $q_{2s}\approx Z-1$. The "real $1s$-vacancy orbital" is half-screened by the $1s$ electron in the doublet system, while in the quartet system under investigation here we find that the "virtual $1s$-vacancy orbital" required to prevent a variational breakdown is essentially unscreened by the $1s$ electron. It should also be pointed out that physically it makes sense that the $2s$-vacancy orbital is almost completely screened by the $1s$ electron. Finally the $2p$-vacancy orbital is chosen to be hydrogenic with $n=2$, $l=1$, and F_{2p} is the relevant associated Laguerre polynomial in Eqs. (7)–(9). We find that $q_{2p}\approx q_{2s}$, i.e., the $2p$-vacancy orbital is also approximately fully screened by the $1s$ electron as might be expected on physical grounds. Actually in all the cases studied here, q_{2p} is slightly smaller than q_{2s} (by about $\frac{1}{4}$), indicating that the $2s$-vacancy orbital is screened less by the presence of the $1s$ electron as compared to the $2p$-vacancy orbital.

The final result of Eq. (14) via these saddle-point variation procedures, is a set of optimized antisymmetrized basis functions Φ_i and optimum linear parameters B_i, such that the energy expectation value of the resulting saddle-point wave function Ψ_{SP} is the saddle-point energy E_{SP}, i.e.,

$$\Psi_{SP}=\sum_i B_i\Phi_i \quad \text{where} \quad \frac{\langle\Psi_{SP}|\mathcal{H}|\Psi_{SP}\rangle}{\langle\Psi_{SP}|\Psi_{SP}\rangle}=E_{SP}\ . \tag{16}$$

The saddle-point energies for the $1s3p3p\ ^4P$ and $1s3s3p\ ^4P^\circ$ systems are given in the first columns of Tables I and II, respectively. The $1s3p3p\ ^4P$ wave functions contained seven partial waves and a total of 65 terms for $Z=2$, 55 terms for $Z=3$, 4, and 5, and 63 terms for $Z=6$. The $1s3s3p\ ^4P^\circ$ wave functions were constructed from seven partial waves for $Z=2$–5 and from eight partial waves for the case of $Z=6$; 46 terms were used for $Z=2$, 52 terms for $Z=3$, 4, and 5, and 50 terms for $Z=6$. The optimized q_{nl} values are given in the second columns of these tables. The next three columns contain relativistic and mass polarization corrections to the energy.[12] These corrections were computed via first-order perturbation theory. The first correction corresponds to the relativistic correction to the kinetic energy plus the Darwin term. The second is due to the retardation of the electromagnetic field between the electrons, often referred to as the orbit-orbit correction. The third correction is a nonrelativistic correction referred to as the mass polarization effect. E total is the sum of saddle-point energy and these first-order corrections.

III. RESONANT WAVE FUNCTION-COMPLEX COORDINATES

The considerations discussed in the previous section suggest that the resonance wave function might be expressed as follows:

$$\Psi_R=\psi_c+\psi_o \tag{17}$$

where the closed-channel component is constructed from the saddle-point solution, and the open-channel component is constructed with the use of complex coordinates.

The open-channel wave function is expanded as follows:

$$\psi_o=\mathcal{A}\psi_t(1,2)\sum_k D_k\mathcal{U}_k^L(3)\ . \tag{18}$$

The two-electron target-state wave function ψ_t is the $1s2p\ ^3P^\circ$ state for the case of the $1s3p3p\ ^4P$ system; for the case of $1s3s3p\ ^4P^\circ$, it can be either the $1s2p\ ^3P^\circ$ or $1s2s\ ^3S$ state. These target states are approximated by three partial-wave configuration-interaction wave functions. The convergence of the energy of these target states, along with the nonrelativistic energy of Accad, Pekeris, and Schiff[13] for comparison are given in Tables III and IV. The outgoing electron's wave function is ex-

TABLE III. Convergence of the nonrelativistic energy of the three-partial wave $(1s2p)^3P^\circ$ state (in a.u.).

No. of partial waves	1	2	3	Accad, Pekeris, and Schiff[a]	
No. of terms[b]	6	9	10	Nonrelativistic	Relativistic
He I	−2.131 666	−2.132 387	−2.132 418	−2.133 164	−2.133 278
Li II	−5.025 344	−5.026 591	−5.026 654	−5.027 716	−5.028 278
Be III	−9.172 195	−9.173 691	−9.173 771	−9.174 973	−9.176 752
B IV	−14.570 124	−14.571 763	−14.571 853	−14.573 138	−14.577 510
C V	−21.218 544	−21.220 273	−21.220 371	−21.221 711	−21.230 855

[a]Reference 13.

[b]The number of terms for helium is 5, 8, and 9.

TABLE IV. Convergence of the nonrelativistic energy of the three-partial wave $(1s2s)^3S$ state (in a.u.).

No. of partial waves	1	2	3	Accad, Pekeris, and Schiff[a]	
No. of terms[b]	4	8	9	Nonrelativistic	Relativistic
He I		−2.175 137	−2.175 178	−2.175 229	−2.175 344
Li II	−5.109 360	−5.110 587	−5.110 651	−5.110 727	−5.111 342
Be III	−9.295 610	−9.297 097	−9.297 097	−9.297 167	−9.299 174
B IV	−14.732 227	−14.733 737	−14.733 819	−14.733 897	−14.738 898
C V	−21.419 010	−21.420 584	−21.420 672	−21.420 756	−21.431 270

[a]Reference 13.
[b]The number of terms for He I is 3, 6, and 7; the number of terms for Li II is 4, 7, and 8.

panded in terms of the one-dimensional complete set of functions $\mathcal{U}_k^L$ which employ complex coordinates in order to represent this continuum electron by a square-integrable function.[14] This basis has the form

$$\mathcal{U}_k^L(j)=r_j^k e^{-\gamma_o r_j} Y_L(\hat{\mathbf{r}}_j)\alpha(\sigma_j) \quad \text{with } r_j \rightarrow r_j e^{-i\theta} , \tag{19}$$

where γ_o is a nonlinear variational parameter. When Eq. (19) is used in Eq. (18) the proper angular and spin coupling is implemented to form the ^4L symmetry of interest; this coupling of $\mathcal{U}$ to the target ψ_t has only been suppressed in these equations for ease of notation. All of the calculations in this work are carried out by expanding the open channel with 15 $D_k s$; k runs from 0 to 14 for εs electrons and from $k=1$ to 15 for εp electrons.

The closed-channel wave function ψ_c in Eq. (17) is considered at two levels of approximation. The more restrictive case simply uses the saddle-point wave function from Eq. (16) as the closed-channel component, i.e.,

$$\Psi_R^{\text{fixed}}=\psi_c^{\text{fixed}}+\psi_o \quad \text{with } \psi_c^{\text{fixed}}=\Psi_{\text{SP}}=\sum_i B_i\Phi_i . \tag{20}$$

The less restrictive case only utilizes the optimized basis functions from the saddle-point computation to expand the closed-channel component, i.e.,

$$\Psi_R^{\text{flexible}}=\psi_c^{\text{flexible}}+\psi_o \quad \text{with } \psi_c^{\text{flexible}}=\sum_i C_i\Phi_i . \tag{21}$$

The terms fixed and flexible refer to the disposition of the linear parameters B_i and C_i, respectively, in the complex variational procedure

$$\delta\frac{\langle\Psi_R|\mathcal{H}|\Psi_R\rangle}{\langle\Psi_R|\Psi_R\rangle}=0 . \tag{22}$$

The parameters C_i in the flexible resonance trial wave function are determined in this variation along with the D_i in ψ_o, whereas the B_i in the fixed resonance trial wave function are held fixed [fixed to the values determined by the saddle-point computation, Eqs. (14) and (16)] and only the D_i are allowed to vary.

The complex eigenvalue which results from the variation given by Eq. (22) is expressed as $E_r-i(\Gamma/2)$. Γ is the autoionization width due to the Auger decay from the "initial state" ψ_c to the "final state" continuum ψ_o. E_r is the resonance energy via which we define a shift from the saddle-point energy by

$$\Delta=E_r-E_{\text{SP}} . \tag{23}$$

IV. RESULTS AND DISCUSSION—$(1s3p3p)^4P$ STATE

The results for the widths and shifts of the $1s3p3p\ ^4P$ closed-channel resonances are given in Table I. Two results are quoted for both the width and the shift of the $1s3p3p\ ^4P$ system which autoionizes via the $[(1s,2p)^3P,\varepsilon p]^4P$ continuum only. The first set of results quoted for these resonance parameters is obtained with the flexible wave function given by Eq. (21), while the second set of results is obtained with the fixed wave function Eq. (20). These results are substantially different for the case of the He^- ion, however the discrepancy between the two sets of results gets progressively smaller as a function of Z at a very fast rate. More specifically the two results for the width differ by 44%, 11%, 2.7%, 0.93%, and 0.38% for $Z=2$ through $Z=6$. The nature of the two trial wave functions used to obtain these results makes it clear that correlation effects are responsible for this discrepancy. Apparently the open-channel component of the resonance wave function significantly perturbs the closed-channel component from that obtained from the saddle-point method for cases of small Z. This is not surprising when considered in the context of the discussion at the beginning of Sec. II where it was pointed out that electron correlations are enhanced in low-Z systems.

A very interesting question is the following: Specifically how is the closed-channel wave function modified by the presence of the open-channel component. We have investigated this question from the point of view that the closed-channel component of the resonant wave function can still be identified as an inner-shell vacancy state in the cases of small Z. If the major change in the closed-channel component results from a modified vacancy orbital, then this situation can be tested by investigating various closed-channel components of the form given by Eq. (13) with different q values and appealing to the general variational principle of stationary energy. More specifically, the correct vacancy orbital in the context of

the full resonance wave function may not be that chosen by the saddle-point method which restricts itself to isolated inner-shell vacancy states which are not perturbed by the continuum.

These ideas are checked out by computing the resonance parameters two different ways with complex coordinates: with the fixed wave function Eq. (20), and also with the flexible wave function Eq. (21); this is done for a range of q values that includes the optimum value generated by the saddle-point method. It should be stressed that when the fixed-type wave function is used with a q value that is not the optimum one chosen by the saddle-point method, the linear parameters B_i and basis functions Φ_i are generated by Eq. (14) using this nonoptimum q. These results are displayed by plotting the resulting resonance energies and widths as a function of q.

Figure 1 plots these resonance energies for the case of He^-; also included in this plot is the energy of the inner-shell vacancy state as a function of q, the maximum of which is the saddle-point energy. The resonance energy yielded by the flexible wave function is stationary over a very wide range of q values as compared to the other energies. This might be expected on the basis of the complex-rotation method with a basis set which is approximately complete. The energy yielded by the flexible wave function takes on a minimum value $-2.065\,037$ a.u. at $q_{2p}=1.04$. The resonance energy yielded by the fixed wave function is stationary over a much smaller range of q values; a minimum $-2.065\,084$ a.u., is found at $q_{2p}=1.14$. The stationary resonance energies from these two methods differ by only 0.000 047 a.u. These resonance energies are both negatively shifted from the saddle-point energy $-2.064\,499$ a.u., this shift being generated by the interaction of the closed- and open-channel components of the resonance wave function. The optimum q values for these resonances energies are somewhat larger than the 0.98 optimum q_{2p} value determined by the saddle-point method which yields a maximum energy for the inner-shell vacancy state. The presence of the open-channel component has the effect of decreasing the amount of shielding of the nucleus experienced by the $2p$-vacancy orbital.

The corresponding He^- widths generated by the two resonance wave functions are plotted in Fig. 2 as functions of q_{2p}. The width from the flexible wave function remains nearly constant for a wide range of q values as might be expected once again based on the theory of the complex-rotation method utilizing a large near-complete basis. On the other hand, the width from the fixed wave function grows fast with increasing q_{2p}. An incorrect value for the autoionization width would clearly be obtained if the width result from the fixed wave function with the saddle-point closed channel were chosen. However, if the fixed-type wave function were opted for and in addition a search for a stationary energy as a function of q were made, then the corresponding width result for $q_{2p}=1.14$ would be chosen, i.e., $\Gamma=0.001\,16$ a.u. The "degree of correctness" for this result can only be judged within this particular investigation by comparing this result to that obtained with the flexible wave function. The flexible wave function yields a stationary resonance energy for $q_{2p}=1.04$, the corresponding width result is $\Gamma=0.001\,26$ a.u.; at this point it should be noted that the width from the flexible wave function only increases from 0.001 21 to 0.001 31 a.u. as q increases from the saddle-point optimum value $q_{2p}=0.976$ to 1.14. The hunt for the optimum width result via the fixed wave function would be more gratifying if this width were stationary

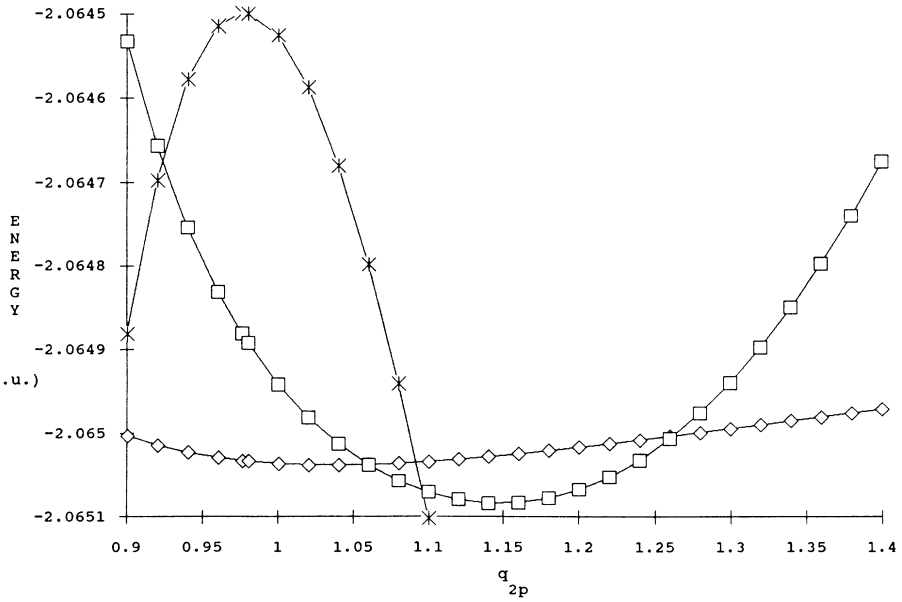

FIG. 1. He^- $1s3p3p\ ^4P$ resonance energy and saddle-point energy as a function of the nonlinear parameter in the vacancy orbital q_{2p}. The energy is expressed in atomic units. * represents the saddle-point energy, see Eqs. (13)–(16); □ represents the resonance energy from fixed-type wave function, see Eqs. (20) and (22); ◇ represents the resonance energy from flexible-type wave function, see Eqs. (21) and (22).

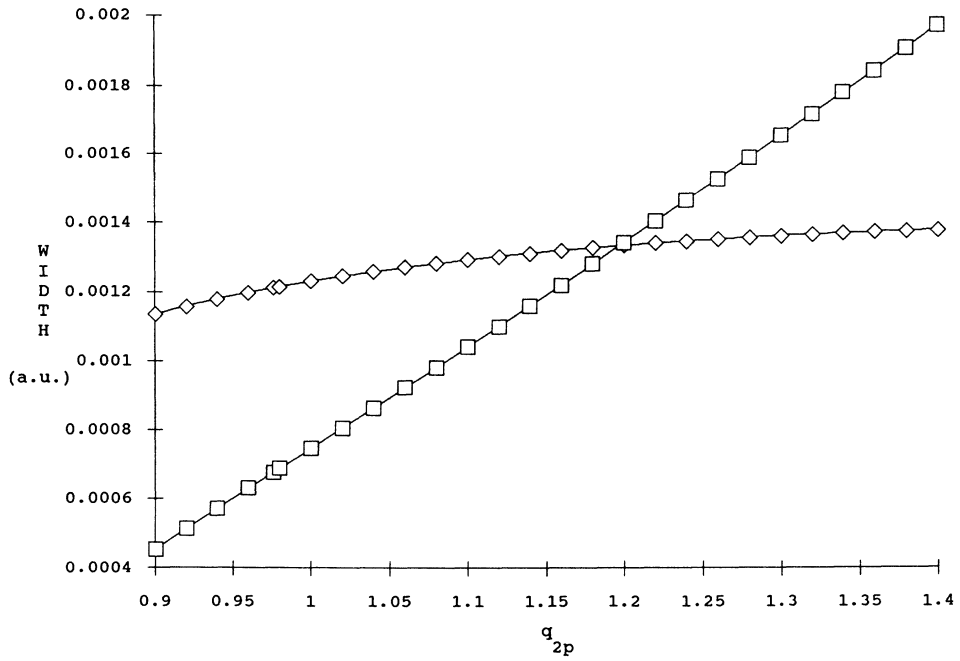

FIG. 2. He^- $1s3p3p\ ^4P$ width as a function of the nonlinear parameter in the vacancy orbital q_{2p}. The width is expressed in atomic units. □ represents the width from fixed-type wave function, see Eqs. (20) and (22); ◇ represents the width from flexible-type wave function, see Eqs. (21) and (22).

along with the energy for the same q value. Inspection of Fig. 2 however does not appear to reveal even a point of inflection for $q_{2p}=1.14$. The corresponding analysis for the case of the lithium atom will be made next where a point of inflection in the width is observed at the q value for which the fixed wave function achieves minimum energy.

The $1s3p3p\ ^4P$ energies for the lithium atom are plotted as functions of q in Fig. 3. The inner-shell vacancy state Eq. (13) acquires maximum energy at $q_{2p}=1.9885$ yielding the saddle-point energy $-4.846\,703$ a.u. The flexible and fixed resonance wave functions take on minimum resonance energies $-4.846\,713$ and $-4.846\,995$ a.u, respectively, for the q values 1.90 and

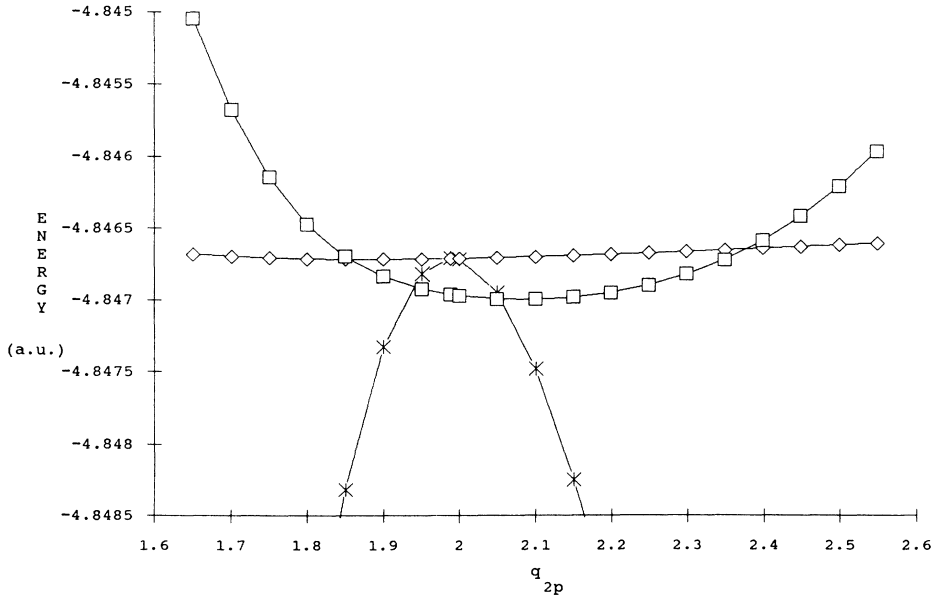

FIG. 3. Li $1s3p3p\ ^4P$ resonance energy and saddle-point energy as a function of the nonlinear parameter in the vacancy orbital q_{2p}. The energy is expressed in atomic units. * represents the saddle-point energy, see Eqs. (13)–(16); □ represents the resonance energy from fixed-type wave function, see Eqs. (20) and (22); ◇ represents the resonance energy from flexible-type wave function, see Eqs. (21) and (22).

2.10. The minimum in the flexible wave function's resonance energy is not detectable at the scale used in Fig. 3; this energy is essentially constant over the full range of q values plotted, varying only by 10^{-4} a.u. The shift of the resonance energy from the saddle-point energy Δ is essentially zero for this neutral atomic system, where it was negative for the negative He^- ion and positive for the positive ions as seen in Table I.

The corresponding lithium $1s3p3p\ ^4P$ widths generated by the two resonance wave functions are plotted in Fig. 4. The same general features that were observed for the He^- system are also present for the case of the lithium atom; i.e., the flexible width is essentially constant as a function of q, while the width from the fixed wave function is a strongly increasing function of q. The width from the fixed wave function is stationary where it agrees with the width from the flexible wave function. More specifically there is a point of inflection for the width near $q_{2p}=2.10$ where the corresponding resonance energy takes on its minimum value. If we accept the width result from the flexible wave function as correct 0.004 60 a.u., then the width from the fixed wave function 0.004 61 a.u. (where both the energy and width are stationary with respect to q) is very good.

The same energy and width analysis was made for $Z=6$. The results for the resonance energy and width from the fixed wave function are found to be more stable (as compared to the lithium results using the same scale for energy and q) as a function of q near the minimum in the energy. The minimum in the resonance energy of the fixed wave function is also found to occur at a q value which agrees more closely with that determined by the saddle-point energies q value, i.e., $q_{2p}=5.00$ versus $q_{2p}=5.024$. This minimum and therefore optimum resonance energy from the fixed wave function is also closer to the optimum energy from the flexible wave function. The conclusion derived from this analysis is that as the correlation effects become weaker for larger values of the nuclear charge Z, the saddle-point inner-shell vacancy state more accurately approximates the closed-channel component of the full resonance wave function. This situation is desirable from a practical point of view since it is much more efficient to optimize q in the context of the inner-shell vacancy state where the Hamiltonian matrix to be diagonalized is real symmetric (i.e., Hermitian) rather than complex symmetric (i.e., non-Hermitian) as is the case when an open channel is added to the basis via complex coordinates. Another very important computer time-saving consideration here is that in the fixed-type resonance wave function the closed-channel component is treated as a single basis element, while in the case of the flexible wave function the closed-channel component must be represented in terms of a large basis; this cuts down on the computer time when the complex-symmetric diagonalization is performed in order to obtain the resonance energy and width.

V. RESULTS AND DISCUSSION— $(1s3s3p)^4P^\circ$ STATE

The results for the widths and shifts of the $1s3s3p\ ^4P^\circ$ closed-channel resonances are given in Table II. This atomic system can autoionize via two distinct open-channel continua, either $[(1s2s)^3S,\varepsilon p]^4P^\circ$ or $[(1s2p)^3P,\varepsilon s]^4P^\circ$. For the case of a narrow Feshbach resonance with multiple decay channels we assume that the distinct decay channels can be treated individually in separate calculations in order to obtain the partial au-

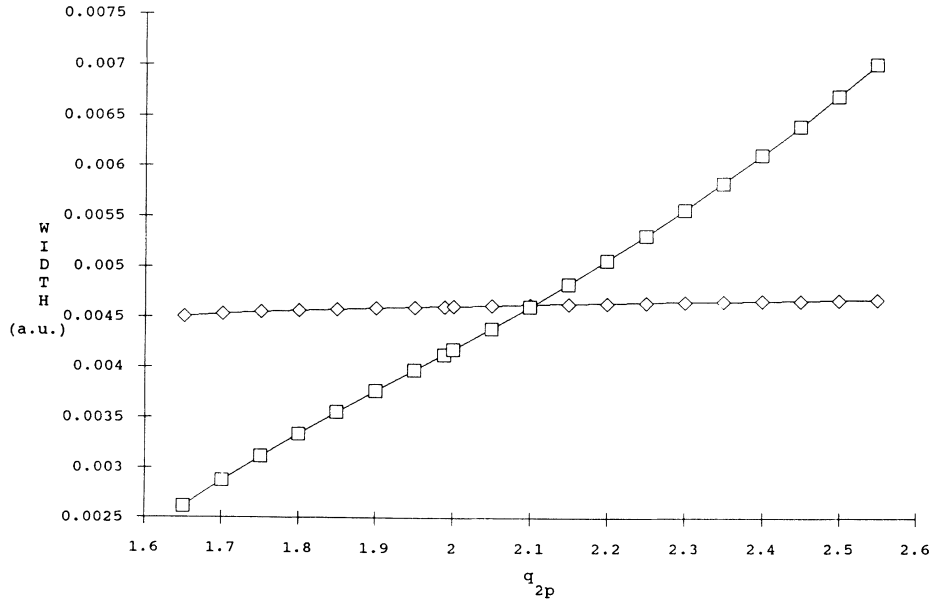

FIG. 4. Li $1s3p3p\ ^4P$ width as a function of the nonlinear parameter in the vacancy orbital q_{2p}. The width is expressed in atomic units. □ represents the width from fixed-type wave function, see Eqs. (20) and (22); ◇ represents the width from flexible-type wave function, see Eqs. (21) and (22).

toionizing widths. The total width due to autoionization is then simply the sum of the transition probabilities or partial widths for the two distinct channels,[15] i.e.,

$$\Gamma=\Gamma_S+\Gamma_P \ . \tag{24}$$

Γ_S is the partial width for autoionization via the $[(1s2s)^3S,\varepsilon p]^4P^\circ$ continuum, while Γ_P is the partial width for radiationless decay via the $[(1s2p)^3P,\varepsilon s]^4P^\circ$ continuum.

Also generated in the complex diagonalization are partial shifts from the saddle-point energy: Δ_S from the $[(1s2s)^3S,\varepsilon p]^4P^\circ$ continuum and Δ_P from the $[(1s2p)^3P,\varepsilon s]^4P^\circ$ continuum. The Auger energies of the ejected electrons in Table II are then computed by

$$\varepsilon_S=E_{\text{total}}+\Delta_S+\Delta_P-E(1s2s\ ^3S) \ , \tag{25}$$

$$\varepsilon_P=E_{\text{total}}+\Delta_P+\Delta_S-E(1s2p\ ^3P^\circ) \ . \tag{26}$$

The relativistic target state energies for the $1s2s\ ^3S$ and $1s2p\ ^3P$ states are from Accad, Pekeris, and Schiff[13] and are given in Tables III and IV, respectively. The shifts employed in these equations were computed via the flexible wave functions. These Auger energies are quoted in electron volts in Table II. The conversion from atomic energy units for a system with nuclear mass $\mathcal{M}$ is

$$1 \text{ a.u.}=2\mathcal{R}_\infty\left[\frac{\mathcal{M}}{\mathcal{M}+m}\right] \tag{27}$$

where m is the electronic mass and $\mathcal{R}_\infty$ is the infinite mass Rydberg 13.605 698 eV.[16] The Auger energies for the $1s3p3p\ ^4P$ states were computed according to Eq. (26) (with $\Delta_S=0$).

The agreement between the widths computed from the flexible and fixed wave functions is very good (less than a 1% difference), except for the case of autoionization to the $[(1s2p)^3P^\circ,\varepsilon s]^4P^\circ$ continuum of He^-. Since there is good agreement between the widths calculated for autoionization to the $[(1s2s)^3S,\varepsilon p]^4P^\circ$ continuum of He^-, it appears that an open channel based on the $1s2p\ ^3P^\circ$ target system is effective in perturbing the closed-channel component for cases of small Z and an open channel based on the $1s2s^3S$ target system is not. It would be interesting to check these ideas out by performing an analysis of the $1s3s3p\ ^4P^\circ$ energy and widths as a function of the vacancy orbitals as was done for the $1s3p3p\ ^4P$ system; however, the computer time involved in such an analysis prohibits it. The projections involved in the $1s3s3p\ ^4P^\circ$ system are more numerous and difficult as compared to the $1s3p3p\ ^4P$ system.

VI. SUMMARY OF METHOD AND RESULTS

The resonance energies and widths of the $1s3s3p\ ^4P^\circ$ and $1s3p3p\ ^4P$ Feshbach resonances were calculated via the saddle-point complex-rotation method. The atomic systems investigated were the negative He^- ion ($Z=2$), neutral atomic lithium ($Z=3$), and the positive ions Be II, B III, and C IV ($Z=4,5,6$).

The $1s3p3p\ ^4P$ state undergoes Coulombic autoionization through the $[(1s2p)^3P,\varepsilon p]^4P$ continuum. The transition rate to this continuum or equivalently the width was obtained by computing the complex eigenvalue $E-i(\Gamma/2)$. The closed-channel component of this resonance wave function was considered at two different levels of approximation: first, it was taken to be the corresponding inner-shell vacancy state computed by the saddle-point method, while in the second case the closed channel was expanded in terms of a large optimum basis set determined by the saddle-point method. The second case has the advantage that the open-channel component can influence the structure of the closed-channel component during the diagonalization of the non-Hermitian Hamiltonian matrix. We found that the $1s3p3p\ ^4P$ width results obtained by these two methods differ substantially from each other for $Z<4$. This discrepancy was attributed to correlation effects in the small-Z systems, where the presence of the open-channel component perturbed the closed-channel component from the form it has as an isolated inner-shell vacancy state (i.e., with no continuum present). This conjecture was investigated theoretically and it was found that the vacancy orbitals were slightly perturbed by the open channel from the form determined by the saddle-point optimization procedure.

With respect to assessing the merit of the real-space saddle-point solution as a candidate for the closed-channel component of a resonance wave function, the analysis carried out in this work has shown that it depends on the degree of the interaction between the closed and open channels and the magnitude of the correlation effects. The analysis performed here was based on two mathematical points: the theory of complex coordinates or complex rotation, and the general variational principle of stationary energy inherent in quantum theory. These two guiding principles show that for most of the states considered here, especially for positive ions, the saddle-point solution is an excellent approximation to the closed-channel component of the resonance wave function. However, in some cases ($1s3p3p\ ^4P$ for He^- and Li, and $1s3s3p\ ^4P^\circ$ interacting with $[(1s2p)^3P,\varepsilon s]^4P^\circ$ for He^-) the closed-channel component is perturbed from the form supplied by the saddle-point method. The analysis implemented here showed that the autoionization width is a strong function of the closed-channel wave function. Therefore, in the cases where the closed channel is perturbed from the saddle-point solution, a width computation with the flexible-type wave function [see Eq. (21)] is in order, or a search for a stationary energy should be made with a wave function of the fixed type [see Eq. (20)]. Even when the fixed-type wave function is used in a complex-coordinate computation, the open-channel component is calculated via the full resonance wave function allowing for correlations to affect it. It should be pointed out that a "golden-rule approach" to the computation of the width should yield a poor result in these cases where correlation effects are important; this is because the initial and final states are computed separately with no mechanism to allow for correlations between these states.

The $1s3s3p\ ^4P^\circ$ system autoionizes via both the $[(1s2s)^3S,\varepsilon p]^4P^\circ$ and $[(1s2p)^3P^\circ,\varepsilon s]^4P^\circ$ open-channel

continua. For this atomic system, we compute the partial widths due to autoionization to the two continua separately, then the total autoionization width is obtained by adding the partial widths. The transition rate to the $[(1s2p)^3P^\circ,\varepsilon s]^4P^\circ$ continuum 0.0013 a.u. is five times larger as compared to the transition rate to the $[(1s2s)^3S,\varepsilon p]^4P^\circ$ continuum for the He^- ion. This larger rate is comparable to the Auger rate from the $1s3p3p\ ^4P$ state to the $[(1s2p)^3P,\varepsilon p]^4P$ continuum for He^-. The $1s3s3p\ ^4P^\circ$ Auger rate to $[(1s2p)^3P^\circ,\varepsilon s]^4P^\circ$ increases monotonically as a function of Z to 0.0016 a.u. for $Z=6$, while the rate to $[(1s2s)^3S,\varepsilon p]^4P^\circ$ increases from 0.000 26 a.u. for He^- to 0.000 98 a.u. for Li then it increases less rapidly to 0.0014 a.u. for $Z=6$. Therefore the decay rates to these two channels is much more equitable for larger Z.

In 1973, Oberoi and Nesbet[17] did an electron-helium scattering calculation. They found a $^4P^\circ$ Feshbach resonance located 0.18 eV below their computed $1s3s\ ^3S$ threshold of 22.69 eV. The width was found to be 0.05 eV. In this work, the $1s3s3p\ ^4P^\circ$ state of He^- is 0.192 eV below the experimental $1s3s\ ^3S$ threshold (22.718 eV) with a width of 0.042 eV. It appears that the $^4P^\circ$ resonance seen by Oberoi and Nesbet should be this $1s3s3p\ ^4P^\circ$ resonance. Our energy is substantially lower mainly because of the extra correlations included in our wave function.

The major decay mode for these states is autoionization. Radiative transitions rates to the lower quartet states are small because of the small energy difference between these states and those of the lower quartets such as $1s2s3p\ ^4P^\circ$, $1s2p3p\ ^4P$, and $1s2s3s\ ^4S$. The radiative electric-dipole transition rate T in terms of the energy difference ΔE and the oscillator strength f is given in atomic units by

$$T=2\alpha^3(\Delta E)^2 f\ . \tag{28}$$

f is constructed from the dipole matrix element, and α is the fine-structure constant. These radiative transition rates increase along an isoelectronic sequence[18] like Z^4, while the oscillator strength in the first approximation is independent of Z. As an example, we consider the C IV ion where the radiative rates are largest, and in order to obtain an upper bound for these transition rates, we assume $f=1$. The estimated upper bounds for the radiative rates for

$$1s3s3p\ ^4P^\circ \rightarrow 1s2p3p\ ^4P,\ 1s3s3p\ ^4P^\circ \rightarrow 1s2s3s\ ^4S\ ,$$

and

$$1s3p3p\ ^4P \rightarrow 1s2s3p\ ^4P^\circ$$

are 0.000 001 9, 0.000 002 8, and 0.000 002 8 a.u., respectively (1 a.u. corresponds to 4.134×10^{16} sec^{-1}). This estimate clearly shows that the radiative rates are significantly smaller than the autoionization rates. The lifetimes τ of these resonances are therefore to a good approximation given by

$$\tau=(2.419\times10^{-17})/\Gamma\ , \tag{29}$$

where Γ is the autionization width in atomic units and τ is the lifetime in seconds. The lifetimes of these states therefore vary from 4×10^{-15} to 2×10^{-14} sec.

The identification of these autoionizing states has not been made experimentally to our knowledge. The recent advances in the experimental detection of low-energy Auger electrons via ion-atom and ion-foil collisions[19] and zero degree spectroscopy techniques[20] make possible the discovery of these core-excited quartet states. We hope that this is achieved soon, and that other theoretical techniques are applied to the computation of these resonances so that comparisons with this work can be made.

VII. BYLICKI'S CRITICISM AND THE SADDLE-POINT METHOD

Recently Bylicki[21] remarked that in some situations variational breakdown may occur in a saddle-point calculation. In a following paper he derived,[22] based on the Feshbach projection-operator approach, an operator for triply excited three-electron systems. It takes the same form as that of the saddle-point method. The energy from Bylicki's method is always lower than or equal to that of the saddle-point method. Therefore, for systems where Bylicki's method is applicable, it guarantees that variational breakdown will never occur in a saddle-point calculation. More discussion on this point is given in a comparison of Bylicki's method with the saddle-point technique.[23]

The situations Bylicki is concerned about are those resonances which lie between an open channel and a closed channel where the individual electrons in the target states of these two channels have exactly the same principal and orbital quantum numbers but different spin symmetry. For example, the $1s2s2p^2P^\circ$ state of He^- lies between the $1s2s\ ^3S$ and $1s2s\ ^1S$ states of helium. In this case, the $2s$ vacancy is not a vacancy of the entire system. If one only built a $1s$ vacancy in the saddle-point wave function, then the inclusion of a partial wave of the symmetry $[(1sns)^3S,mp]$ will likely cause a variational breakdown in the (real-space) variational calculation. For the systems of interest in this work, the open channels are $1s2s\ ^3S$ and $1s2s\ ^3P$, whereas the closed channels are $1s3s\ ^3S$ and $1s3p\ ^3P$. Here the $2s$ and $2p$ vacancies are present in the entire closed-channel wave function, hence Bylicki's concern does not apply. Furthermore, variational breakdown can only occur in a (real-space) variational calculation when open channels are inadvertently present. It is no longer an issue when open channels are explicitly included to carry out a complex-coordinate calculation such as we have done in this work.

The criticism of Bylicki came as a total surprise, because the saddle-point method does not forbid the building of a certain vacancy in a segment of the total wave function in order to remove an open channel. The open channel can usually be removed in a number of ways.[24] This is obvious to anyone who uses the saddle-point method. An example is the recent work of Jaskolska and Woznicki on $Li[(1s2s)^1S,nd]^2D$ resonances.[25] It appears that they were aware of the generalized saddle-point method of Bylicki's prior to its publication but they still preferred to use the saddle-point method. It should be

evident that if the saddle-point method is properly used, then it will not suffer from variational breakdown.

While our method does not suffer from variational breakdown for the systems mentioned by Bylicki, the corresponding saddle-point energies, however, may not be an excellent approximation for these resonances. (The saddle-point complex-rotation method does not suffer from this weakness.) This is because in these systems the open and closed channels differ by only one electron's orbital. The corresponding shift to the resonance position could be much larger than those systems where the open and closed channels differ by two electron orbitals. For this reason, we have investigated very few systems of this kind using the saddle-point method. For the few systems we have applied it to, we never claimed high precision. Nevertheless, it was the application of the saddle-point method to the $1s2s2p\,^2P^\circ$ state of He^- that first revealed the Feshbach resonance nature of this state.[26] Bylicki claimed that we had left out a partial wave which contributes about 2 meV to the correlation energy of the $^2P^\circ$ state of He^-, and therefore was not negligible. The neglected shift for this state is about 200 MeV.[27]

ACKNOWLEDGMENTS

This work is supported by the National Science Foundation Grant No. PHY-8715238 and by the National Research Council of the Republic of China.

[1]B. F. Davis and K. T. Chung, J. Phys. B **15**, 3113 (1982).
[2]R. Bruch, D. Schneider, K. T. Chung, B. F. Davis, and N. Stolterfoht, J. Phys. B **20**, L341 (1987).
[3]B. F. Davis and K. T. Chung, Phys. Rev. A **37**, 111 (1988).
[4]B. F. Davis and K. T. Chung, Phys. Rev. A **39**, 3942 (1989).
[5]B. F. Davis and K. T. Chung, Phys. Rev. A **31**, 3017 (1985).
[6]K. T. Chung, Phys. Rev. A **20**, 1743 (1979); B. F. Davis and K. T. Chung, *ibid.* **22**, 835 (1980).
[7]K. T. Chung and B. F. Davis, in *Autoionization II,* edited by A. Temkin (Plenum, New York, 1985), p. 73.
[8]M. H. Chen, in *Atomic Inner-Shell Physics,* edited by B. Crasemann (Plenum, New York, 1985), p. 67.
[9]Landau and Lifshitz, *Quantum Mechanics Non-relativistic Theory,* 3rd ed. (Pergamon, New York, 1977), p. 278.
[10]K. T. Chung, Phys. Rev. A **39**, 5483 (1989).
[11]Richard Liboff, *Introductory Quantum Mechanics* (Addison-Wesley, Reading, MA, 1980), p. 397.
[12]K. T. Chung and B. F. Davis, Phys. Rev. A **29**, 1871 (1984).
[13]Y. Accad, C. L. Pekeris, and B. Schiff, Phys. Rev. A **4**, 516 (1971).
[14]B. F. Davis and K. T. Chung, Phys. Rev. A **36**, 1948 (1987); C. W. McCurdy, in *Resonances,* edited by D. G. Truhlar (American Chemical Society, Washington, DC, 1984), p. 25.
[15]C. W. McCurdy and T. N. Rescigno, Phys. Rev. A **20**, 2346 (1979).
[16]E. R. Cohen and B. N. Taylor, Report of the CODATA Bulletin No. 63 (Pergamon, New York, 1986).
[17]R. S. Oberoi and R. K. Nesbet, Phys. Rev. A **8**, 2969 (1973).
[18]R. D. Cowan, *The Theory of Atomic Structure* (University of California Press, Berkeley, 1981), p. 438.
[19]M. Agentoft, T. Anderson, K. T. Chung, and B. F. Davis, Phys. Scr. **31**, 74 (1985).
[20]R. Bruch, N. Stolterfoht, S. Datz, P. D. Miller, P. L. Pepmiller, Y. Yamazaki, H. F. Krause, J. K. Swenson, K. T. Chung, and B. F. Davis, Phys. Rev. A **35**, 4114 (1987).
[21]M. Bylicki, Phys. Rev. A **39**, 3316 (1989).
[22]M. Bylicki, Phys. Rev. A **40**, 1748 (1989).
[23]K. T. Chung (unpublished).
[24]K. T. Chung, Phys. Rev. A **41**, 4090 (1990).
[25]B. Jaskolska and W. Woznicki, Phys. Scr. **39**, 230 (1989); **39**, 234 (1989).
[26]K. T. Chung, Phys. Rev. A **23**, 1079 (1981).
[27]P. G. Burke, J. W. Cooper, and S. Ormonde, Phys. Rev. **183**, 245 (1969); B. R. Junker, J. Phys. B **15**, 4495 (1982).